Proceedings of the 6th International Conference on Gas Hydrates (ICGH 2008),
Vancouver, British Columbia, CANADA, July 6-10, 2008.

THE USE OF HORIZONTAL WELLS IN GAS PRODUCTION FROM HYDRATE ACCUMULATIONS

George J. Moridis*, Matthew T. Reagan and Keni Zhang
Earth Sciences Division
Lawrence Berkeley National Laboratory
1 Cyclotron Rd., MS 90-1116, Berkeley, California
USA

ABSTRACT

The amounts of hydrocarbon gases trapped in natural hydrate accumulations are enormous, leading to a recent interest in the evaluation of their potential as an energy source. Earlier studies have demonstrated that large volumes of gas can be readily produced at high rates for long times from gas hydrate accumulations by means of depressurization-induced dissociation, using conventional technology and vertical wells. The results of this numerical study indicate that the use of horizontal wells does not confer any practical advantages to gas production from Class 1 deposits. This is because of the large disparity in permeabilities between the hydrate layer (HL) and the underlying free gas zone, leading to a hydrate dissociation that proceeds in a horizontally dominant direction and is uniform along the length of the reservoir. When horizontal wells are placed near the base of the HL in Class 2 deposits, the delay in the evolution of a significant gas production rate outweighs their advantages, which include higher rates and the prevention of flow obstruction problems that often hamper the performance of vertical wells. Conversely, placement of a horizontal well near to top of the HL can lead to dramatic increases in gas production from Class 2 and Class 3 deposits over the corresponding production from vertical wells.

Keywords: gas hydrates, gas production, horizontal wells

NOMENCLATURE

A	Reservoir surface area [m^2]
HL	Hydrate layer
FL	Fluids layer
k	Intrinsic permeability [m^2]
M_w	Cumulative mass of produced water [kg]
P	Pressure [Pa]
Q_{avg}	Average gas production rate [ST m^3/s]
Q_H	Wellbore heating rate [W/wellbore m]
Q_M	Mass rate of fluids production [kg/s]
Q_P	Gas production rate [ST m^3/s]
Q_R	Gas release rate [ST m^3/s]
Q_w	Water mass production rate [kg/s]
r,z	Cylindrical coordinates [m]
R_{max}	Radius of cylindrical reservoir (m)
t	Time (s)
T	Temperature [^oC]
S_A	Aqueous phase saturation
S_{irA}	Irreducible aqueous phase saturation
S_G	Gas phase saturation
S_{irG}	Irreducible gas phase saturation
S_H	Hydrate phase saturation
V_G	Cumulative volume of free gas in reservoir [ST m^3]
V_P	Cumulative volume of produced gas [ST m^3]
V_R	Cumulative volume of released gas [ST m^3]
x,y,z	Cartesian coordinates [m]
Δz	Discretization along the z-axis [m]
ΔZ_F	Fluids layer thickness [m]
ΔZ_H	Hydrate layer thickness [m]
ΔZ_O	Overburden thickness [m]
ΔZ_U	Underburden thickness [m]
ΔZ_W	Well position below the HL [m]
ϕ	Porosity

INTRODUCTION

Background

Gas hydrates are solid crystalline compounds in which gas molecules (referred to as guests) occupy the lattices of ice-like crystal structures called hosts [1]. Hydrate deposits occur in two distinctly different geographic settings where the necessary conditions of low T and high P exist for their

* Corresponding author: Phone: (510) 486 4746 Fax (510) 486 5686 E-mail: GJMoridis@lbl.gov

formation and stability: in the permafrost and in deep ocean sediments. The majority of naturally occurring hydrocarbon gas hydrates contain CH_4 in overwhelming abundance. There has been no systematic effort to map and evaluate this resource on a global scale [2], and current estimates of in-place volumes vary widely (ranging between 10^{15} to 10^{18} ST m^3), but the consensus is that the worldwide quantity of hydrocarbon gas hydrates is vast [1,3,4]. Even if a conservative estimate is considered and only a small fraction is recoverable, the sheer size of the resource is so large that it demands evaluation as a potential energy source. The appeal of hydrates is enhanced by an ever-increasing global energy demand and the environmental desirability of natural gas.

Although formidable difficulties exist, the development of hydrates into an energy source appears to have acquired its own global dynamic, with increased levels of international awareness, several national and international programs investigating the feasibility of the endeavor, and heightened levels of activity [2]. Of the three possible methods of hydrate dissociation [5] for gas production (i.e., depressurization, thermal stimulation, and use of inhibitors), depressurization appears to be the most efficient [2,7,8]. Recent studies [6,7,8,9] have indicated that, under certain conditions, gas can be produced from natural hydrate deposits at high rates over long periods using conventional technology. Practically all of these investigations involved vertical wells, but preliminary results from an early horizontal well study offered some tantalizing possibilities [8].

Objectives and approach

The objective of this study is to assess the performance of horizontal wells in gas production from the three main classes of hydrate deposits. The evaluation approach involves comparison of the characteristics of gas production from horizontal wells to those from single vertical wells for which production data have been previously published (reference cases). Figure 1 shows a schematic of the horizontal well system, in addition to its most important geometric parameters. In this study, the hydrate-forming gas is assumed to be 100% CH_4, and the conditions are identical in the vertical and horizontal well studies, as are the areas of the corresponding production units (well spacing) and the amounts of hydrate included therein. All the simulations were conducted using the serial and parallel versions of the TOUGH+HYDRATE code [10].

PRODUCTION FROM CLASS 1 DEPOSITS

Class 1 accumulations are composed of two layers: the hydrate layer (hereafter referred to as HL) and an underlying fluids layer (FL), i.e., a two-phase fluid zone containing free (mobile) gas and liquid water. In this class, the bottom of the hydrate stability zone (i.e., the location above which hydrates are stable because of thermodynamically favorable P and T conditions) coincides with the bottom of the hydrate interval. The study of Moridis et al. [11] on production from such deposits provided the reference cases.

Production from Class 1W deposits: Cases A-x

These hydrate deposits involve coexistence of hydrate and water in the HL, which is possible only if the capillary pressure P_{cap} is very strong [11]. Note that such strong P_{cap} is unlikely in the coarse sediments of hydrate deposits that are usually associated with desirable production targets. We investigated the following cases:

Reference Cases A-V1 and A-V2. The most important properties and conditions in the Reference Case A-V1 are listed in Table 1. In the HL, $S_H = 0.7$ and $S_A = 0.3$. In the underlying FL, $S_H = 0.7$, and S_A and S_G are determined from P_{cap}. The fluids production rate $Q_M = 0.555$ kg/s corresponds to 0.82 ST m^3/s (= 2.5 MMSCFD) when 100% gas is produced. The 10 m long producing interval, completed in the gas zone, is electrically heated at a rate of $Q_H = 500$ W per meter of wellbore to prevent the formation of secondary hydrate (and flow blockage) inside the wellbore. The cylindrical reservoir radius $R_{max} = 564.2$ m, corresponding to an area (well spacing) of $A = 100$ ha (250 acres). The domain was discretized in 90x94 = 8,460 cells in (r,z). The radial discretization is logarithmic and the vertical discretization is variable, with $\Delta z = 0.25$ m in the HL [11]. The reader is directed to [11] for a detailed description of the problem. In Case A-V2, Q_M is double that of Case A-V1.

Case A-H1: The rectangular permafrost deposit in Case A-H1 belongs to the same formation as the reference cases A-V1 and A-V2 (i.e., the same stratigraphy and characteristics along the z-axis), and has the same $A = 100$ ha. The square footprint of the deposit results in a well length $L_y = 1000$ m. Because of symmetry, only a single slice of unit thickness and $L_x = 500$ m is simulated. The horizontal well is placed immediately below the HL, with $\Delta Z_w = 0.125$ m. Thus, the domain is discretized into 180x94 = 16,920 cells in (x,z), with the discretization along the z- axis being identical to that of the reference cases. The wellbore is heated at a rate of $Q_H = 100$ W/m, and the $Q_M = 2.775 \times 10^{-4}$ kg/s is identical with that of Case A-V1 when summed over the entire domain.

Case A-H2: Here $Q_M = 5.55 \times 10^{-4}$ kg/s, i.e., double that of Case A-H1 and equal to that of Case A-V2 when summed over the entire domain.

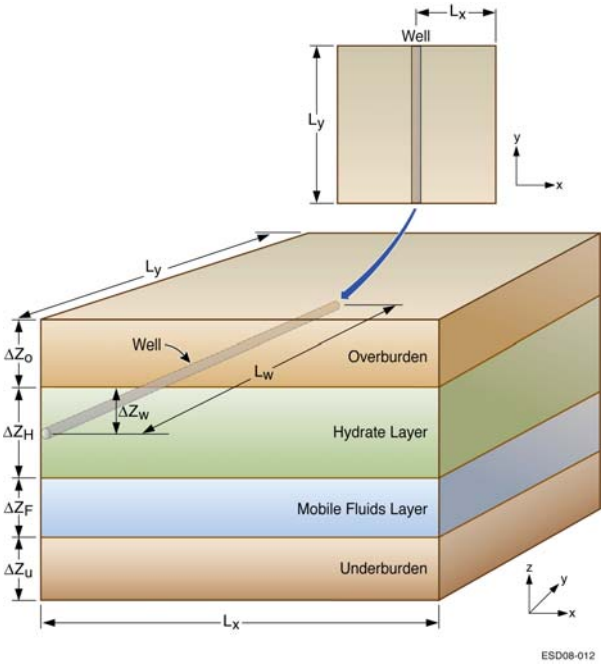

Figure 1: Horizontal well configuration

Parameter	Value
Overburden thickness ΔH_O	30 m
HL thickness ΔH_H	15 m
FL thickness ΔH_F	15 m
Underburden thickness ΔH_U	30 m
Initial pressure P (at HL base)	1.067×10^7 Pa
Initial temperature T (HL base)	286.65 K
Geothermal gradient	0.029 K/m
HL/FL permeability $k_r=k_z$ in (r,z), or $k_x= k_y =k_z$ in (x,y,z)	4.34×10^{-13} m^2
Overburden/underburden k	0 m^2
HL/FL porosity ϕ	0.3
Overburden/underburden ϕ	0
Fluid production rate Q_M	0.555 kg/s
Dry thermal conductivity $k_{\Theta d}$	0.5 W/m/K
Wet thermal conductivity $k_{\Theta w}$	3.0 W/m/K
Irreducible gas saturation S_{irG}	0.02
Irreducible aqueous sat. S_{irA}	0.25
All other properties	See [11]

Table 1. Properties and conditions in Case A-V1

Case A-H3: This study differs from Case A-H1 in the location of the horizontal well, which is now placed at ΔZ_w = 5 m below the HL base.

Horizontal well performance in Class 1W deposits

To quantitatively describe gas production from Class 1 hydrates, we use the concepts of *Rate Replenishment Ratio* (RRR) and *Volume Replenishment Ratio* (VRR) [11]. The term RRR = Q_R/Q_P, and describes the fraction of the gas production rate Q_P that is replenished by CH_4 released from hydrate dissociation. Similarly, VRR = V_R/V_P, and defines the fraction of the cumulative volume of produced gas that is replenished by hydrate-originating CH_4. These two parameters provide a measure of the hydrate system response and the effectiveness of dissociation as a gas-producing method [11].

Figure 2 shows the RRR for all A-x cases, and indicates that, for a given Q_M, the use of a horizontal well (Cases A-H1, A-H2 and A-H3) does not enhance hydrate dissociation and confers practically no benefits to gas production from hydrate deposits. For the case of lower Q_M (Cases A-H1 and A-H3), RRR is about 0.5 at t = 3 years, with horizontal wells resulting in somewhat higher RRR (not exceeding 15%), indicating higher contributions of gas released from dissociation to gas production from horizontal wells. For the higher Q_M (Case A-H2), the improvement in the RRR of horizontal well is initially practically negligible, and, after reaching a peak RRR = 0.4, the trend shifts toward significant deterioration for t > 470 days. This is caused by hydrate lensing (Figure 3) and the occlusion of the dissociating interfaces by very high S_H levels promoted by the high P_{cap} [11].

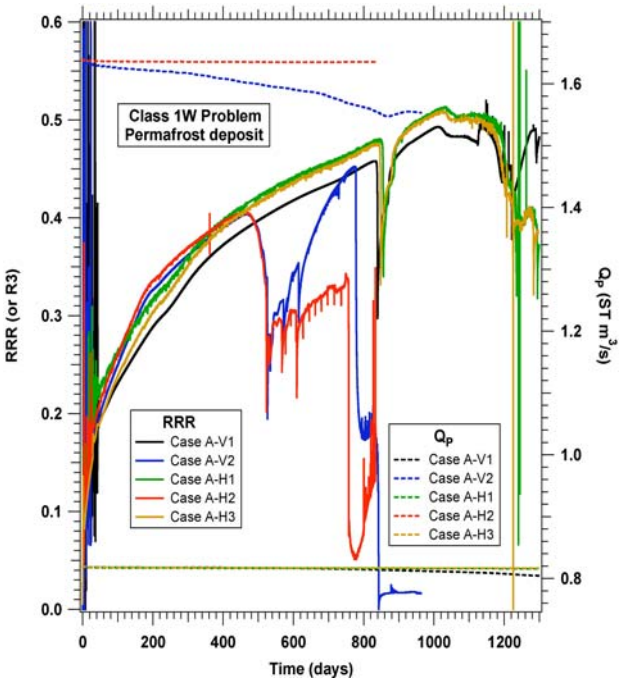

Figure 2: RRR and Q_P during gas production from Class 1W permafrost deposits (Cases A-x)

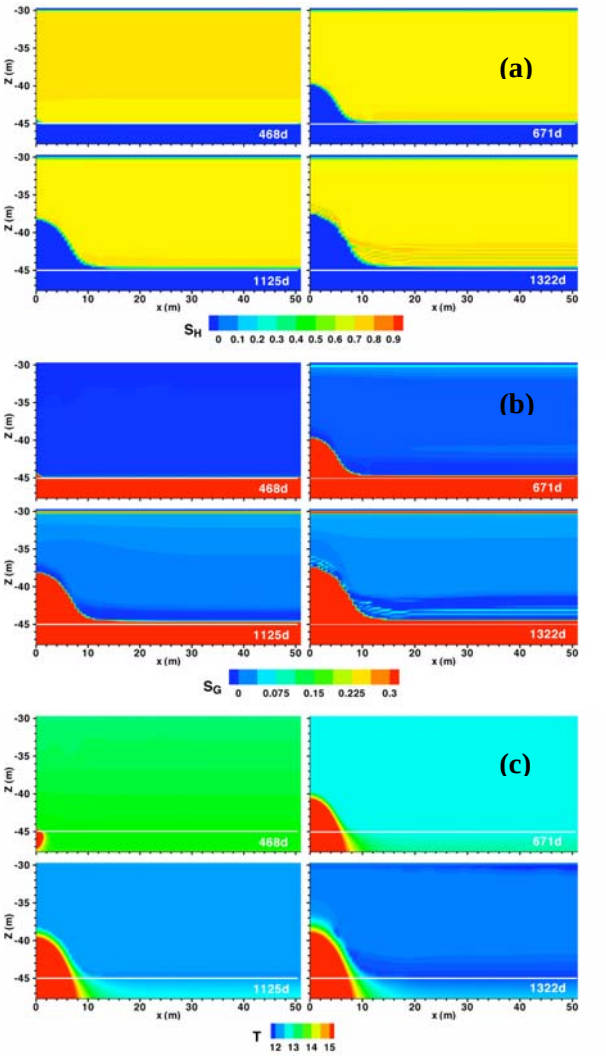

Figure 3: Evolution of the (a) S_H, (b) S_G, and (c) T distributions near the well in Case A-H1.

The deterioration in the horizontal well performance at a higher Q_M negates the slight benefit from the higher Q_P (indicating lower Q_w from horizontal wells). Of interest is Case A-H3, which indicates that positioning the horizontal well deeper within the FL does not have any practical effect on performance. The slightly lower RRR value is attributed to less effective depressurization caused by the larger ΔZ_w, which is incapable of preventing hydrate lensing and a decrease in dissociation [11].

Such lensing is evident near the receding dissociation interface at the bottom of the HL in Figures 3a and 3b, which also show (a) hydrate destruction in the vicinity of the well, (b) a gradual decrease in S_H in the rest of the hydrate body, and (c) the evolution of the upper dissociation interface, a typical feature of depressurization-induced dissociation in all classes of hydrate deposits [6,7,10]. The evolution of the spatial distributions of S_G and T in Figures 3b and 3c is entirely analogous to the ones for vertical wells, and shows the development of a gas bank at the top of the HL and the gradual cooling of the hydrate body, because of the endothermic nature of the dissociation reaction.

Figure 2 indicates that the RRR patterns of the horizontal wells very closely track those corresponding to the vertical-well cases, although the results represent very different coordinate systems and discretizations. The remarkable similarities include the onset and evolution of the various dissociation stages identified in [10], and tend to indicate that the horizontal and vertical well solutions both capture accurately physical phenomena, as opposed to numerical artifacts.

The observations from Figure 2 are confirmed in Figure 4, which fails to show anything more than practically insignificant gains (especially at higher Q_M) when horizontal wells are used for gas production from Class 1W deposits. The somewhat higher VRR for a low Q_M is easily within the range of uncertainty in the values of the dominant parameters. The only advantage of horizontal wells appears to be the generally lower Q_w (Figure 5), but this is very low in absolute terms and thus confers no practical benefit.

Production from Class 1G deposits: Cases B-x

These hydrate deposits involve coexistence of hydrate and gas in the HL, and are likely to be more common than Class 1W deposits. We investigated the following cases:

Reference Cases B-V1 and B-V2. The properties and conditions in Case B-V1, while very similar to those in Case A-V1, differ in the following aspects:

(a) In the HL, $S_H = 0.7$ and $S_G = 0.3$.
(b) The permeability $k = 4.34 \times 10^{-14}$ m^2
(c) $Q_H = 200$ W/wellbore m
(d) P_{cap} is much milder (see [10])

In Case B-V2, Q_M is double that of Case B-V1.

Case B-H1: This case is the Class 1G equivalent of Class A-H1, to which it is entirely analogous. Thus, the rectangular permafrost deposit in Case B-H1 belongs to the same formation as the reference cases B-V1 and B-V2, and its geometry and discretization are the same as in Case A-H1. Apart from the initial phase saturations in the HL, the only difference between Cases A-H1 and B-H1 is that there is no wellbore heating in the latter.

Case B-H2: Here $Q_M = 5.55 \times 10^{-4}$ kg/s, i.e., double that of Case B-H1 and equal to those of Cases B-V2 and A-V2 when summed over the entire domain.

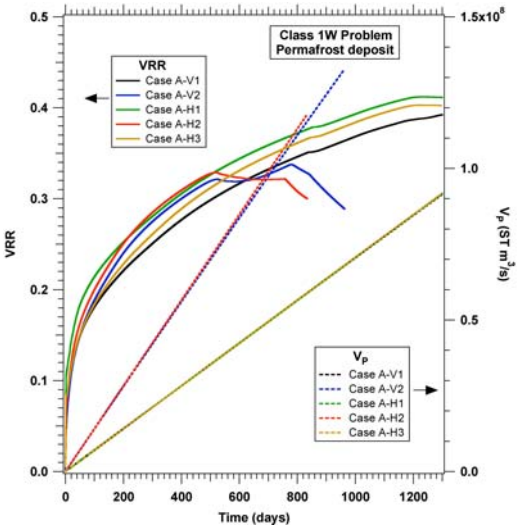

Figure 4: VRR and V_P during gas production from Class 1W permafrost deposits (Cases A-x)

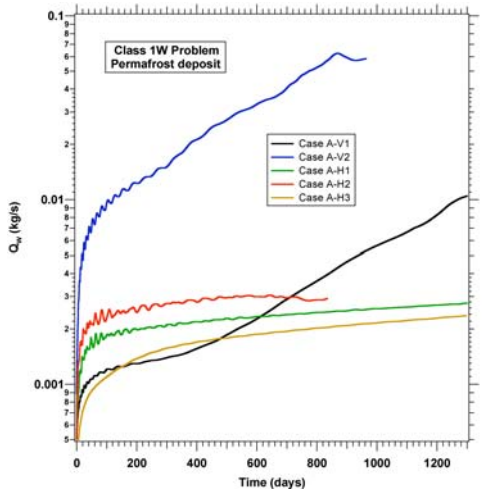

Figure 5: Evolution of Q_w during gas production from Class 1W permafrost deposits (Cases A-x)

Horizontal well performance in Class 1W deposits

Figure 6 shows the RRR for all B-x cases and indicates that, for a given Q_M, the use of a horizontal well (Cases B-H1 and B-H2) does not enhance hydrate dissociation and confers practically no benefits to gas production from hydrate deposits. The corresponding VRR shows the same behavior. These results are entirely consistent with the observations of the horizontal well performance in Class 1W deposits.

As in the Class 1W problems, horizontal wells appear to result in lower water production (Figure 7). However, this is no real advantage because the water production is very low in absolute terms.

Horizontal wells in Class 1 deposits: Synopsis of observations

The results of this numerical study indicate that, because, because of the very large disparity in effective permeability between the HL and the FL, hydrate dissociation proceeds in a horizontally dominant direction and is uniform along the length of the reservoir. Consequently, the use of horizontal wells placed below the base of the HL does not lead to long-term increases in the rate of gas production or in the total volume of recoverable gas. The obvious conclusion is that, in gas production from Class 1 hydrate deposits, the easier-to-install vertical wells are just as effective as the much more expensive horizontal wells.

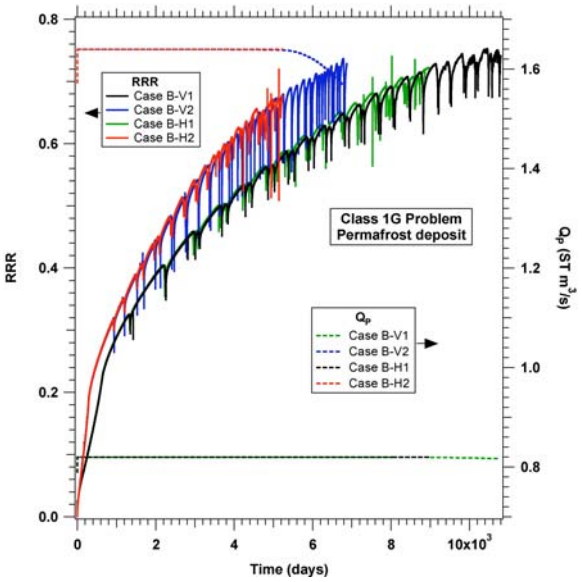

Figure 6: RRR and Q_P during gas production from Class 1G permafrost deposits (Cases B-x)

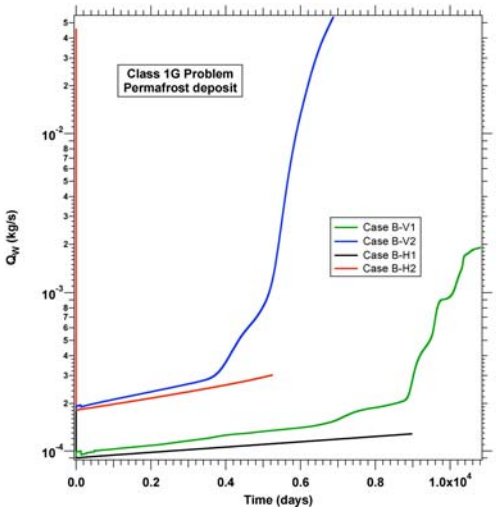

Figure 7: Evolution of Q_w during gas production from Class 1G permafrost deposits (Cases B-x)

PRODUCTION FROM CLASS 2 DEPOSITS

Class 2 accumulations are composed of two layers: the Hydrate Layer (hereafter referred to as HL) and an underlying Fluids Layer (FL) that is fully saturated by water. In this class, the bottom of the hydrate stability zone may be at or below the bottom of the hydrate interval. The study of Moridis and Reagan [6] on production from Class 2 oceanic deposits representative of the Tigershark formation in the Gulf of Mexico provided the reference cases.

Class 2 cases to be considered

These hydrate deposits invariably involve coexistence of hydrate and water in the HL. We investigated the following cases:

Reference Cases C-V1, C-V2 and C-V3. The most important properties and conditions in the reference Case C-V1 are listed in Table 2. Cases C-V1 and C-V2 use the new well design [6] that involves (a) initially (Phase 1) a 5 m production interval beginning at the HL base and completed in the FL from, with a heated outer wellbore surface in the entire HL, (b) warm water injection near the top of the HL and extension of the production interval into the receding HL during production in Phase 2, and (c) alternating intervals of warm water injection and production during the last (depletion) phase of production. This well design was shown to maximize gas production by allowing an open pathway between the upper dissociation interface and the well [6]. Case C-V3, corresponding to the "Short Production Interval" well concept [6], involves a 5 m production that begins at the HL base, is completed entirely within the FL, and involves no heating. It is included in the discussion because it is the most direct analogue of the horizontal well Case C-H3.

The cylindrical reservoir radius R_{max} = 800 m, corresponding to an area (well spacing) of A = 200 ha (500 acres). The domain was discretized in 119x113 = 13,447 cells in (r,z). The radial discretization is logarithmic, and the vertical discretization is variable, with Δz = 0.25 m in the HL [6]. The reader is directed to [6] for a detailed description of the problem. In Case C-V2, Q_M is double that of Case C-V1.

Case C-H1: The rectangular permafrost deposit in Case C-H1 belongs to the same formation as the reference cases and has the same stratigraphy, the same characteristics along the z-axis, and the same A = 200 ha. The square footprint of the deposit results in a well length L_y = 1414 m. Because of symmetry, only a single slice of unit thickness and L_x = 707 m is simulated. The domain is discretized into 200x113 = 22,600 cells in (x,z), with the discretization along the z-axis being identical to that of the reference cases. The horizontal well is placed at the top of the HL and is not heated. Production proceeds in two stages: a short (30-day) period during which the well is produced at a constant bottomhole pressure P_w = 2.7 MPa, followed by a long period (to the exhaustion of the hydrate) of production at a constant mass rate of $Q_M = 6.703\text{x}10^{-3}$ kg/s. This Q_M is identical to that of Case C-V1 when summed over the entire domain. The short constant-P_w stage is needed to develop an open (hydrate-free) pathway between the horizontal well at the top of the HL and the underlying aquifer, without which it is next to impossible to produce at the desired Q_M.

Case C-H2: The same two-stage production process employed in Case C-H1 is used here, but Q_M in the second stage is double that of Case C-H1, and equal to that of Case C-V2 when summed over the entire domain.

Case C-H3: This case does not involve the two-stage production process used in Cases C_H1 and C-H2. Instead, fluids are produced from a horizontal well placed immediately below the HL (i.e., at the top of the aquifer in FL) at a constant rate of $Q_M = 6.703\text{x}10^{-3}$ kg/s. This case is the horizontal well analogue of case C-V3.

Parameter	**Value**
Overburden thickness ΔH_O	30 m
HL (aquifer) thickness ΔH_H	18.25 m
FL thickness ΔH_F	15 m
Underburden thickness ΔH_U	30 m
Initial pressure P (at HL base)	$3.3\text{x}10^7$ Pa
Initial temperature T (HL base)	294.15 K
Initial saturations in the HL	S_H=0.7 S_A=0.3
Initial saturations in the FL	S_A=1
Water salinity (mass fraction)	0.03
Geothermal gradient	0.03464 K/m
HL/FL permeability k_r=k_z in (r,z), or k_x= k_y =k_z in (x,y,z)	$7.5\text{x}10^{-13}$ m^2
Overburden/underburden k	0 m^2
HL/FL porosity ϕ	0.3
Overburden/underburden ϕ	0
Fluid production rate Q_M	18.955 kg/s (10,000 BPD)
Dry thermal conductivity $k_{\Theta d}$	0.5 W/m/K
Wet thermal conductivity $k_{\Theta w}$	3.0 W/m/K
Irreducible gas saturation S_{irG}	0.02
Irreducible aqueous sat. S_{irA}	0.25
All other properties	See [6]

Table 2. Properties and conditions in Case C-V1

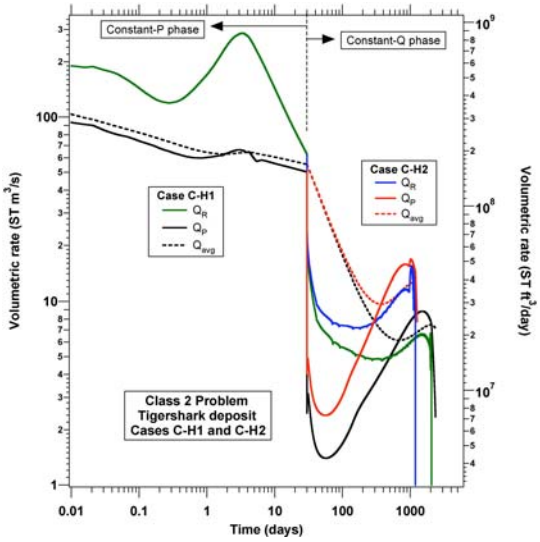

Figure 8: Horizontal well performance in Class 2 deposits (Cases C-H1 and C-H2)

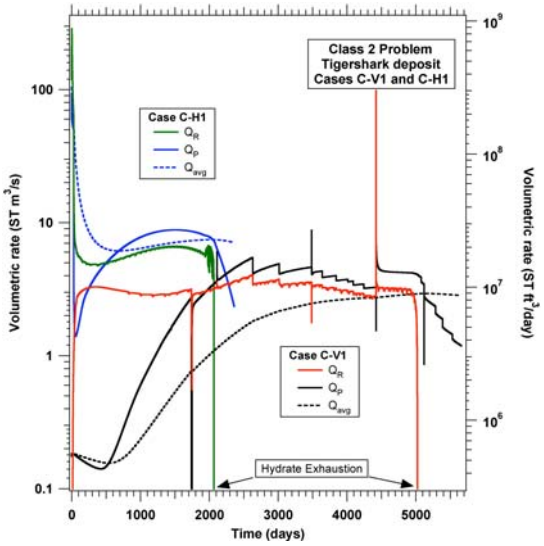

Figure 9: Comparison of horizontal and vertical well performance (Cases C-V1 and C-H1)

Horizontal well performance in Class 2 deposits

The effectiveness of horizontal wells in gas production from Class 2 deposits is amply demonstrated by Figure 8, which shows the evolution of Q_P and Q_R in Cases C-H1 and C-H2. Additionally, Figure 8 shows the running average of the gas production rate, defined as $Q_{avg} = V_P/t$. Very high gas production is observed during the first stage (constant-P_w) of production, with Q_P ranging between 100 and 52.5 ST m^3/s (300 to 180 MMSCFD). The corresponding Q_R is even higher, and indicates a near-explosive gas release in the reservoir. Q_P declines initially at the beginning of the second (constant-Q_M) stage, but then increases continually. Thus, Q_P declines to levels as low as 1.5 and 2.4 ST m^3/s in Cases C-H1 and C-H2, respectively (4.6 and 7.3 MMSCFD), but reaches levels as high as 8.8 and 17 ST m^3/s (27 and 52 MMSCFD, respectively). At the time of the exhaustion of the hydrate (denoted in Figure 8 by a zero Q_R), Q_{avg} in Cases C-H1 and C-H2 is 7.2 and 12.8 ST m^3/s, respectively (22 and 39 MMSCFD). These results are consistent with earlier observations from single vertical-well systems [6], which had indicated that gas production increases with Q_M. Thus, the highest sustainable Q_M level should be employed for maximum production.

The superiority of horizontal wells in gas production from Class 2 deposits is clearly demonstrated in Figure 9, which shows a comparison between the well performances in Cases C-V1 and C-H1. Q_P and Q_{avg} in Case C-H1 are consistently larger (always significantly, and often orders of magnitude) than those in Case C-V1.

At the time of the hydrate exhaustion, Q_{avg} in Case C-V1 is about 2.6 ST m^3/s (7.9 MMSCFD), i.e., about 3 times lower than that for Case C-H1. The reduction of the time to hydrate exhaustion from about 5,000 to 2,070 days (and the corresponding increase in well productivity) makes horizontal wells particularly attractive. Their appeal is further enhanced by the observation that the two-stage production strategy in cases C-H1 and C-H2 is free of the long lead-time of low Q_P that characterizes production from vertical wells.

Secondary hydrate formation during production from vertical wells can lead to flow blockage (thus requiring the complex well configuration with localized heating in case C-V1), and may necessitate the reductions in Q_M that are shown in Figure 9 [6]. Another advantage of horizontal wells is the prevention of this problem even without wellbore heating. The reason is the longer well length, which reduces (a) gas flow velocities in the vicinity of the well bore, (b) the corresponding Joule-Thomson cooling, and, thus, (c) the tendency to form secondary hydrates. This is demonstrated in the S_H distribution of Figure 10, which shows no secondary hydrates near the well. Note the hydrate-free pathway connecting the top of the HL (where the well is located) and the aquifer at t = 30 days, i.e., the end of the constant-P_w stage. This indicates that this stage is sufficiently long for the dissociation front moving outward from the well to reach the FL.

Figure 10, and the corresponding S_G distributions in Figure 11, shows the typical features of depressurization-induced dissociation during gas production from hydrate reservoirs:

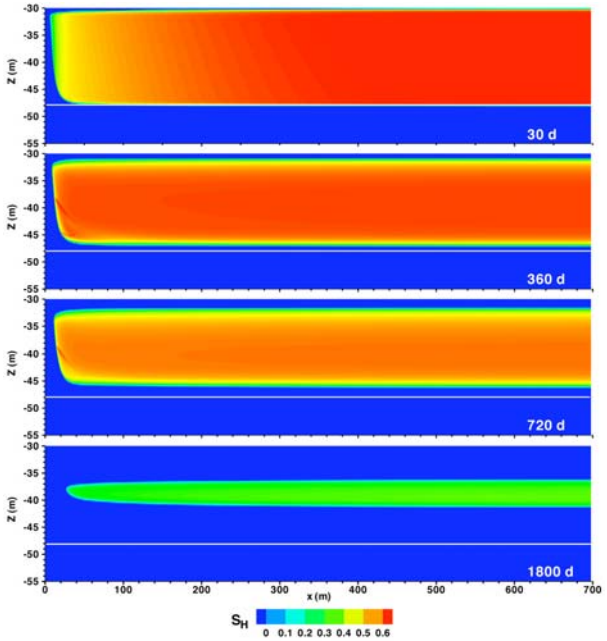

Figure 10: Evolution of the S_H distribution in the hydrate deposit of Case C-H1.

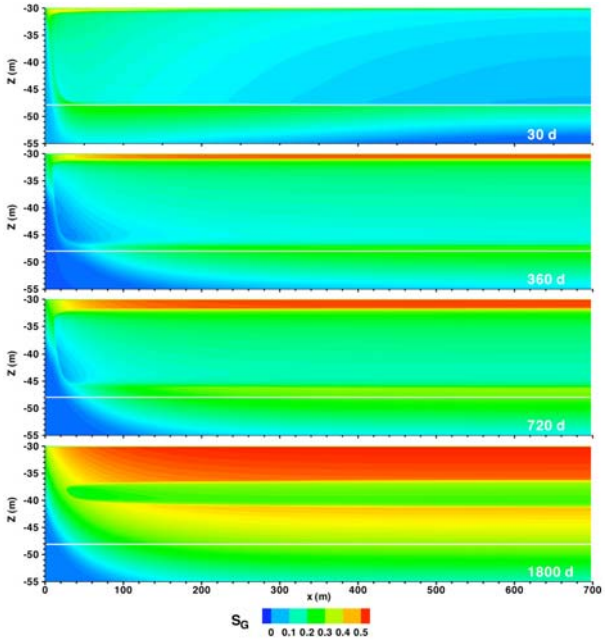

Figure 11: Evolution of the S_G distribution in the hydrate deposit of Case C-H1.

(a) the evolution of an upper dissociation interface at the HL top that moves downward; (b) gas accumulation at high S_G at the top of the hydrate-free zone below the overburden, in addition to a gas bank underneath the shrinking hydrate body; and (c) a dissociation pattern that is remarkably uniform along the length of the deposit.

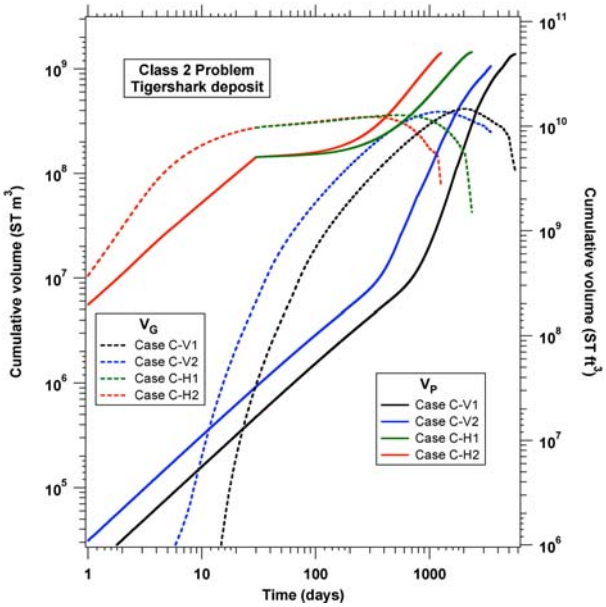

Figure 12: Evolution of the V_P and V_G in the Class 2 hydrate deposit

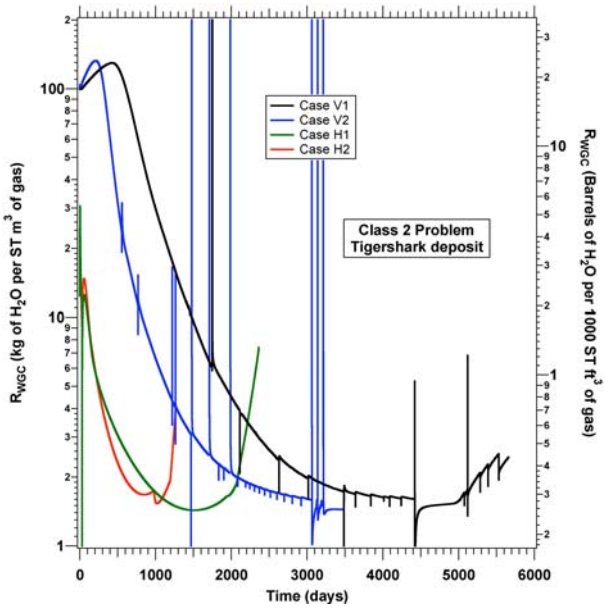

Figure 13: Evolution of the R_{WGC} in the Class 2 hydrate deposit

The cumulative volumes V_P and V_G in Figure 12 show that the use of horizontal wells results in early production of large gas volumes, and early accumulations of large volumes of gas in the reservoirs, thus providing additional evidence of the superiority of horizontal wells in Class 2 deposits. Further confirmation is provided by the water-to-gas ratio $R_{WGC}=M_w/V_P$ in Figure 13, which shows that horizontal wells result in consistently

better R_{WGC} than the corresponding vertical wells. In horizontal wells, R_{WGC} begins to deteriorate (indicating increasing production of the water released from accumulation that had been draining and accumulating in the reservoir) after the exhaustion of the hydrate. The location of the well at the top of the HL allows easy access to the location of the largest gas accumulation (Figure 11) and sufficient separation from the water. The rapidly rising R_{WGC} is associated with low pressures, and can serve as a criterion for the cessation of operations and abandonment of the reservoir.

The effect of the location of the well and of the corresponding production strategy is clearly demonstrated in Figure 14, which shows the Q_R and Q_P in Cases C-V3 and C-H3. Here, the horizontal well is located immediately below the HL (i.e., at the top of the aquifer), and is produced continuously at a constant Q_M. For consistency in the comparison, Figure 14 shows the corresponding performance of the vertical well in Case C-V3. The use of the horizontal well is shown to be substantially superior to the vertical well and leads to a large Q_P without any need to resort to reductions in Q_M and the danger of cessation of production (a clear possibility in Case C-V3). However, these advantages are overshadowed by a long initial lead period of low Q_P. This is about 50% longer than that for the vertical well of Case C-V3, indicating a waiting period of over 2 years before the onset of rapid gas production. The reason for this delay is the less-focused depressurization in the horizontal well system (as Q_M is distributed over a much longer well length), which requires longer times to develop a sufficiently large bank of mobile gas such that gas production can begin in earnest. The larger localized depressurization is the reason for the earlier response of the vertical well in Case C-V3.

PRODUCTION FROM CLASS 3 DEPOSITS

Class 3 accumulations are composed of a single HL bounded by near-impermeable formations and have no underlying zone of mobile fluids, i.e., $\Delta Z_F = 0$. As is also the case in Class 2 deposits, the bottom of the hydrate stability zone in Class 3 accumulations may be at or below the bottom of the hydrate interval. The study of Moridis and Reagan [7] on production from Class 3 oceanic deposits representative of the Tigershark formation in the Gulf of Mexico provided the reference cases.

Class 3 cases to be considered

Class 3 hydrate deposits invariably involve coexistence of hydrate and water in the HL. We investigated the following cases:

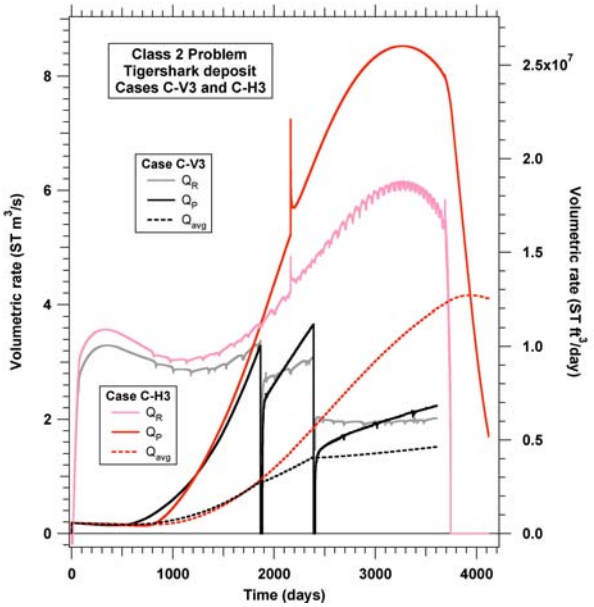

Figure 14: Comparison of horizontal and vertical well performance (Cases C-V3 and C-H3)

Reference Case D-V. This problem is identical to that in Case C-V1, from which it differs in that $\Delta Z_F = 0$. This is accomplished by assigning to the FL from Case C-V1 the properties of the impermeable underburden, thus resulting in $\Delta Z_F = 45$. This allows the use of the data input files from the C-1V runs and eliminates any need for development of a new grid and initialization (both laborious processes). An additional difference involves the production method and the well construction. The well is now completed in the entire hydrate interval and is produced at a constant $P_w = 2.7$ MPa. A thorough discussion of the specifics of Case D-V can be found in [7].

Case D-H: Similarly, Case D-H is treated as a variation of Case C-H1, and uses the same grid and discretization after the minor adjustments described in the discussion of case D-V.

Horizontal well performance in Class 3 deposits

Figure 15 shows the evolution of Q_P, Q_R and Q_{avg} in Cases D-V and D-H, and clearly demonstrates the effectiveness of horizontal wells in gas production from Class 3 deposits. The initial gas release is practically explosive, beginning with Q_P = 100 ST m^3/s (305 MMSCFD) at t = 1 day, then continuously declining to 25 ST m^3/s (75 MMSCFD) at t = 200 days, and to 2 ST m^3/s (6 MMSCFD) at t = 1,440 days, when the hydrate is almost depleted. Consistent with the behavior of Class 3 deposit under constant-P_w depressurization, Q_R is initially higher than Q_P, but the two become practically equal for $t > 200$ days.

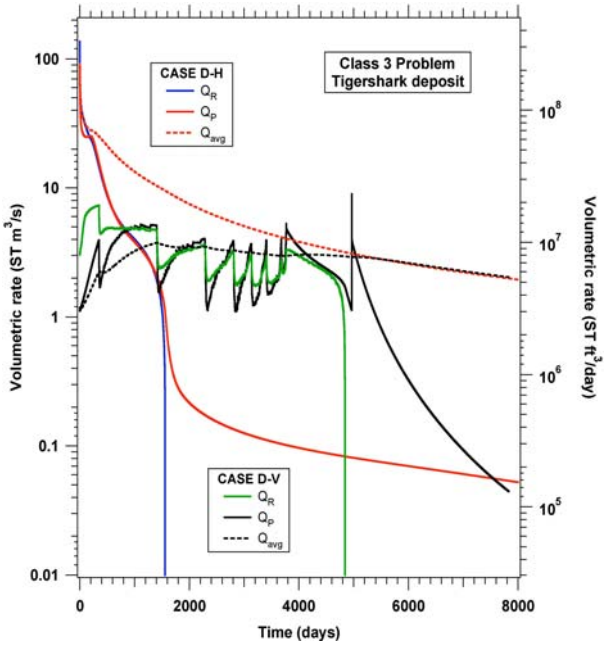

Figure 15: Comparison of horizontal and vertical well performance (Cases D-V and D-H)

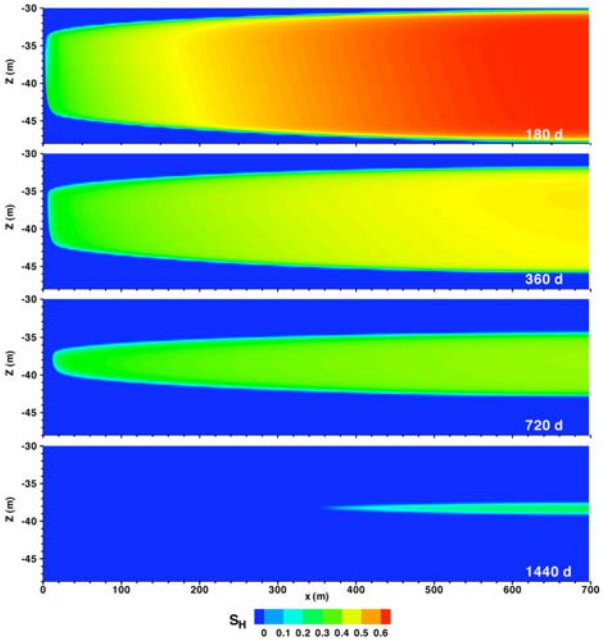

Figure 16: Evolution of the S_H distribution in the hydrate deposit of Case D-H.

Q_P and Q_{avg} in Case D-H are consistently larger (always significantly, and often by orders of magnitude) than those in Case D-V. At the time of the exhaustion of the hydrate (denoted in Figure 15 by a zero Q_R), Q_{avg} in Cases D-V and D-H is 3 and 10.2 ST m^3/s (9 and 30.6 MMSCFD), respectively. As in the study of the Class 2 deposits, the reduction of the time to hydrate exhaustion from about 4,500 to 2,440 days (and the corresponding increase in well productivity) makes horizontal wells particularly attractive.

Their appeal is further enhanced by the observation that horizontal wells appear to be free of the problem of significant secondary hydrate formation in the reservoir, which can lead to flow blockages (such as the "dual traveling barriers" discussed in [7]) and are responsible for the oscillatory behavior of Q_P and Q_R over time (Figure 15). This is demonstrated by the smoothness of the Q_P and Q_R curves in Figure 15. It is also clearly depicted by the S_H distribution of Figure 16, which shows no secondary hydrates near the well. As was the case in the study of the Class 2 deposit, Figure 16, and the corresponding S_G and T distributions in Figures 17 and 18, exhibits the characteristics of depressurization-induced dissociation in hydrate deposits: the evolution of an upper dissociation interface and gas accumulation at the top of the HL, a gas bank underlying the receding body of hydrate, a continuously declining T where hydrates dissociate, and a remarkable spatial uniformity in the hydrate dissociation pattern.

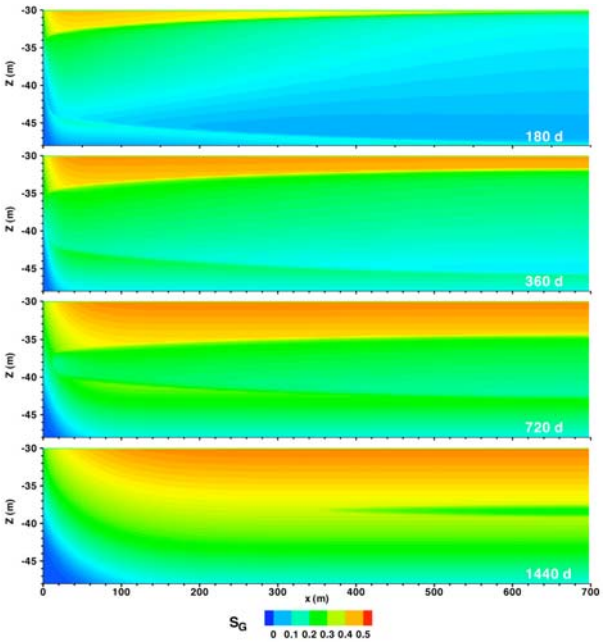

Figure 17: Evolution of the S_G distribution in the hydrate deposit of Case D-H.

The cumulative volumes V_R and V_P in Figure 19 show that the use of horizontal wells results in an early release and production of large gas volumes. This is not accompanied by the accumulation of significant amounts of gas in the reservoir, as the evolution of V_G indicates (Figure 18). Actually, the gas accumulation is smaller than in the Case D-V

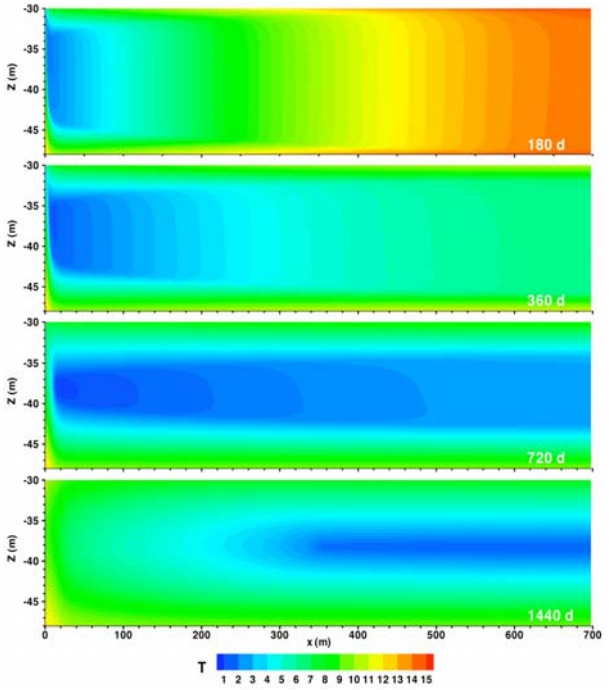

Figure 18: Evolution of the T distribution in the hydrate deposit of Case D-H.

of the vertical well. This is because the easier access to the long horizontal wellbore does not promote gas accumulation in Case D-V. Conversely, the need of the gas to travel the entire distance from the boundaries to the single vertical well at the center of the reservoir results in longer residence times and the gas accumulation pattern of Case D-V.

Further confirmation of the effectiveness of horizontal wells in production from Class 3 deposits is provided by the water-to-gas ratio R_{WGC} in Figure 20, which shows that horizontal wells result in consistently better R_{WGC} than the corresponding vertical wells. The location of the well at the top of the HL allows easy access to the accumulated gas at the top of the reservoir (Figure 17) and delays water production. The arrival of the water that has been accumulating in the reservoir at the well is marked by a sudden deterioration in R_{WGC}, as evidenced by the sudden increase in its value. Similar to the Class 3 deposit case, this deterioration in R_{WGC}, coupled with the corresponding economic and technical considerations (such as low reservoir pressure) may serve as a criterion to trigger a decision to abandon production from the deposit.

CONCLUSIONS

The following conclusions can be drawn from this study:

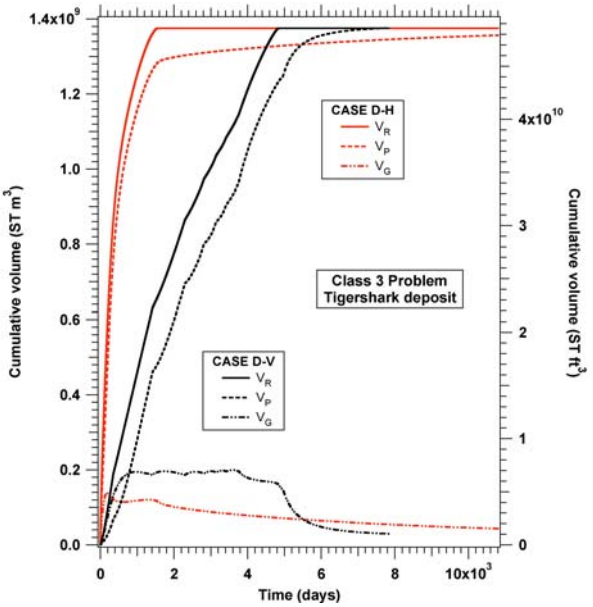

Figure 19: Evolution of the V_R, V_P and V_G in the Class 3 hydrate deposit (Cases D-V and D-H)

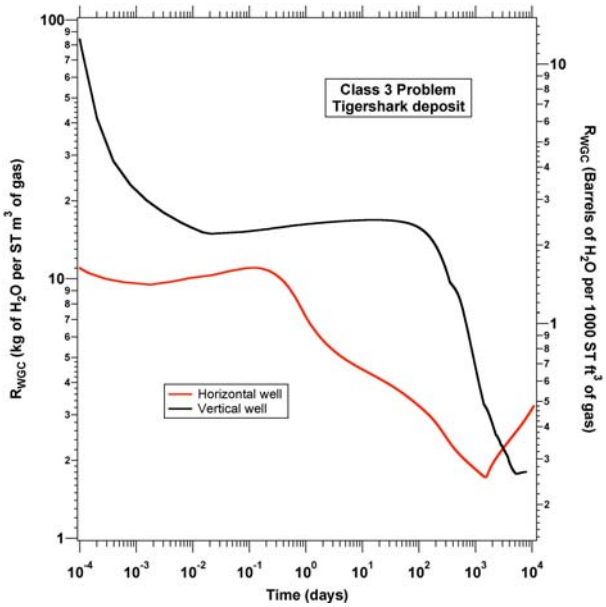

Figure 20: Evolution of the R_{WGC} in the Class 3 hydrate deposit (Cases D-V and D-H)

(1) The use of horizontal wells does not confer any practical advantages to gas production from Class 1 deposits because of the very large disparity between the permeability in the HL and in the FL. This leads to a hydrate dissociation pattern that proceeds in a horizontally dominant direction and is uniform along the length of the reservoir. These observations apply to horizontal wells in both Class 1W and 1W deposits. The location of

the horizontal well within the deposit does not appear to have any practical effect.

(2) In terms of production rates, horizontal wells are invariably superior to vertical ones in production from Class 2 deposits. When a horizontal well is placed at the top of the HL and a two-stage production strategy (involving a short constant-P_w production period, followed by a long period of constant-Q_M production), the improvement over the corresponding vertical well production is spectacular. Thus, for a Q_M = 18.955 kg/s (= 10,000 BPD) from the entire reservoir, the average production rate Q_{avg} to the time of hydrate exhaustion increases from 2.6 ST m^3/s (7.9 MMSCFD) to 7.2 ST m^3/s (22 MMSCFD), respectively. When Q_M is doubled, Q_{av} increases to 12.8 ST m^3/s (39 MMSCFD). Note that the instantaneous rates can be much higher.

(3) When horizontal wells are placed near the base of the HL in Class 2 deposits, the production rate eventually reaches levels that are much higher than the ones for the corresponding vertical well system. However, this configuration does not appear particularly useful, because it is accompanied by a significant delay in the onset of significant gas production.

(4) Horizontal wells are invariably superior to vertical ones in production from Class 3 deposits. When a horizontal well is placed at the top of the HL and a constant-P_w production is imposed at the well, the improvement in performance over that of the corresponding vertical well production is dramatic. Thus, for a P_w = 2.7 MPa, the average production rate Q_{avg} to the time of hydrate exhaustion increases from 3 to 10.2 ST m^3/s, (from 9 to 30.6 MMSCFD), respectively. As in the Class 2 case, the instantaneous rates can be much higher.

(5) A significant advantage of horizontal wells in production from Class 2 and Class 3 deposits (and a possible reason for their very encouraging performance) is the prevention of formation of secondary hydrates in the vicinity of the wellbore. Formation of such hydrates is promoted by Joule-Thomson cooling from the large velocities needed to maintain constant-rate flow in vertical wells. The lower gas velocities in horizontal wells appear to alleviate (and possibly eliminate) the problem.

ACKNOWLEDGMENTS

This study was supported by the Assistant Secretary for Fossil Energy, Office of Natural Gas and Petroleum Technology, through the National Energy Technology Laboratory, under the U.S. Department of Energy, Contract No. DE-AC02-05CH11231. The authors are indebted to Stefan Finsterle, John Apps and Dan Hawkes for their thorough review and their insightful comments.

REFERENCES

[1] Sloan, E.D., and C. Koh, Clathrate Hydrates of Nautral Gases. 3rd Edition, Boca Raton, FL: Taylor and Francis, Inc., 2008.

[2] Moridis, G.J., Collett, T.S., Boswell, R., Kurihara, M., Reagan, M.T., Koh, C., Sloan, E.D. *Toward Production From Gas Hydrates: Current Status, Assessment of Resources, and Simulation-Based Evaluation of Technology and Potential.* SPE 114163, 2008 SPE Unconventional Reservoirs Conference, Keystone, Colorado, U.S.A., 10–12 February 2008.

[3] Milkov, A.V. *Global estimates of hydrate-bound gas in marine sediments: how much is really out there?* Earth Science Reviews 2004: 66: 183.

[4] Klauda, J.B., and Sandler, S.I. *Global distribution of methane hydrate in ocean sediment.* Energy and Fuels: 2005: 19: 459.

[5] Makogon, Y.F. Hydrates of Hydrocarbons. Tulsa, OK: Penn Well Publishing Co., 1997.

[6] Moridis, G.J., Reagan, M.T. *Gas Production From Oceanic Class 2 Hydrate Accumulations*, OTC 18866, 2007 Offshore Technology Conference, Houston, Texas, U.S.A., 30 April–3 May 2007.

[7] Moridis, G.J., and Reagan, M.T. *Strategies for Gas Production From Oceanic Class 3 Hydrate Accumulations*, OTC 18865, 2007 Offshore Technology Conference, Houston, Texas, 30 April – 3 May 2007.

[8] Kurihara, M., K. Funatsu, H. Ouchi, Y. Masuda and H. Narita. *Investigation On Applicability Of Methane Hydrate Production Methods To Reservoirs With Diverse Characteristics*. Paper 3003, Proceedings of the 5th International Conference on Gas Hydrates, Trondheim, Norway, 13–16 June: 3: 714-725.

[9] Hong, H., and Pooladi-Darvish, M. *Simulation of Depressurization for Gas Production from Gas Hydrate Reservoirs*, J. Can. Pet. Tech. 2005: 44(11): 39-46.

[10] Moridis, G.J., Kowalsky, M.B., and Pruess, K. TOUGH+HYDRATE v1.0 User's Manual. Report LBNL-0149E, Lawrence Berkeley National Laboratory, Berkeley, CA, 2008.

[11] Moridis, G.J., Kowalsky, M.B., Pruess, K. *Depressurization-Induced Gas Production From Class 1 Hydrate Deposits*, SPE REE 2005: 10(5): 458-481.